

行政院國家科學委員會補助專題研究計畫 成果報告
 期中進度報告

銻化物基材之量子結構及元件 (2/3)
Antimonide based quantum structures and devices

計畫類別： 個別型計畫 整合型計畫

計畫編號：NSC 96-2221-E-009-221-

執行期間： 97 年 8 月 1 日至 98 年 7 月 31 日

計畫主持人：李建平教授 國立交通大學電子工程學系

共同主持人：

計畫參與人員：李定麒、羅明城、蘇聖凱、林岳民

國立交通大學電子工程學系

成果報告類型(依經費核定清單規定繳交)： 精簡報告 完整報告

本成果報告包括以下應繳交之附件：

- 赴國外出差或研習心得報告一份
- 赴大陸地區出差或研習心得報告一份
- 出席國際學術會議心得報告及發表之論文各一份
- 國際合作研究計畫國外研究報告書一份

處理方式：除產學合作研究計畫、提升產業技術及人才培育研究計畫、
列管計畫及下列情形者外，得立即公開查詢

涉及專利或其他智慧財產權， 一年 二年後可公開查詢

執行單位：國立交通大學電子工程學系

中 華 民 國 98 年 5 月 20 日

中文摘要

在本研究中，我們設計了一個新的異質界面場效電晶體元件結構改善銻基電晶體的崩潰電壓。我們選擇使用砷化銻或銻化銻為元件之通道材料。藉由能階工程及量子侷限的概念，我們預期所設計的結構可以同時維持高電子遷移率及增加電晶體的操作崩潰電壓。初期，此結構是成長於半絕緣砷化銻的基板上，並使用厚膜銻化鋁作為材料緩衝層。

更進一步，我們希望可以使這樣的元件可以與成熟之矽積體電路結合，可以使元件可以更廣泛的運用，故吾人同時研究銻化銻材料在矽基板上的磊晶技術，希望可以成長出高品質之銻化銻，我們研究了不同的緩衝層材料對於銻化銻磊晶之影響，第一個樣品完全不使用任何的緩衝層直接將銻化銻成長於矽基板上，第二個樣品使用 100 奈米之銻化鋁作為緩衝層，第三個樣品使用十個週期之銻化銻（10 奈米）/銻化鋁（10 奈米）超晶格做為緩衝層，我們分別研究其低溫光激光譜、X-Ray 晶格繞射及表面原子力顯微鏡分析。在不同的分析技術下，第三個樣品皆呈現最佳的磊晶品質，同時我們利用穿透式電子顯微鏡分析樣品三之晶格缺陷，研究中發現超晶格結構可以有效的阻擋晶格缺陷，故樣品三會具有最佳之結晶品質。

同時，我們亦研究了銻砷化銻成長於砷化銻基板上的銻、砷的組成比例隨著晶格應力變化行為。吾人準備了七種不同厚度之銻砷化銻薄膜之樣品，但是維持其相同之銻及砷之元素分子通量比例，利用 X-Ray 倒晶格對應及離子通道分析技術，吾人定義了銻砷化銻薄膜中銻及砷百分比之變化，因為銻砷化銻對於砷化銻基板具有應力，吾人發現銻及砷百分比的比例會隨著應力的大小而有所變化。在分子束磊晶的成長中，三族成分的百分比，可以精準的從材料的分子通量來做精準的調整，但是五族成分的變化，卻不是如此，本實驗中發現，除了元素分子通量外，晶格應力的變化亦會改變五族的成分比例改變。

關鍵詞： 銻化銻、銻化銻、砷化銻、異質界面場效電晶體

Abstrate

In this work, we proposed a new structure to effectively improve the breakdown problem in Sb-based HFETs. To choose the appropriate materials with both a larger band gap and a lattice constant close to them (InAs, InSb) to enlarge the band gap of channel material is the design challenge. By taking advantage of the band gap engineering, we design the InAs/InAsSb composite channel and expect to realize an InAs channel HFET with both a high mobility and a higher breakdown voltage. The device was grown on the semi-insulator GaAs substrate with thick AlSb buffer layer.

Furthermore, for the integration with the mature silicon base circuit, it is important to realize the HFET device on the silicon substrate. Therefore, the GaSb growth on silicon substrate was also studied. Three samples were prepared with different buffer layer structure. A: without buffer layer. B: with 100nm AlSb buffer layer. C: with ten periods AlSb(10nm)/GaSb(10nm) superlattice buffer layer. By the low temperature photoluminescence, X-Ray diffraction and the surface atomic force microscope analysis, the sample C shows the best result. Also, by the transmission electron microscope study, the superlattice buffer layer is efficient to prevent the dislocation propagation and merge the dislocations.

Also, we investigate the composition profile of GaAsSb grown on GaAs substrates by solid-source molecular beam epitaxy. It's found that the Sb composition fraction grades increasingly instead of keeping constant throughout the GaAsSb epitaxial layer. This is attributed to the strain-induced Sb segregation during the growth of GaAsSb on the GaAs substrate.

Keyword: GaSb, InSb, InAs, HFET

Introduction:

The Sb-based binary compound semiconductor AlSb, GaSb, InSb and InAs together with their related alloys are candidates for high-speed, low power electronic devices. Applications could include high-speed analog and digital systems used for data processing, communications, imaging and sensing, particularly in portable equipment such as hand-held devices and satellites. The development of Sb-based transistors for use in low-noise high-frequency amplifiers, digital circuits and mixed-signal circuits could provide the enabling technology needed to address these rapidly expanding needs. Fig 1 shows the trend toward higher frequencies and lower power consumption with increasing lattice constant [1]. In recent years, considerable progress has been made in Sb-based heterostructure field-effect transistors (HFETs).

However, due to the narrow band gap of InAs (0.36 eV) and InSb (0.18 eV) channel materials, impact ionization effects can become dominant for short gate lengths as drain bias exceeds the energy gap in the channel. Further, because the staggered band lineup at the InAs/AlSb heterojunctions leaves holes without confinement, some of the impact-ionized holes are drawn into negatively bias gate, giving rise to a significant gate leakage component, others accumulate in the buffer layers and induce nonsaturating drain characteristics by the feedback mechanism, known as the kink effects. Proposed approaches to improve breakdown including the use of a back gate [2], increased quantum confinement [3], dual gating [4], additional InAs subchannel [5], composite channel like InAs/InAsP and InAs/InAlAs [6-7] and InAsSb channel [8]. However, the improvement in breakdown voltage is still limited thus far, which will largely limit the allowable device operation range. In this work, we proposed a new solution to effectively improve the breakdown problem in Sb-based HFETs. By taking advantage of the band gap engineering, we designed the InAs/InAsSb composite channel to realize higher breakdown voltage.

The Sb-base electron device was usually realized on the semi-insulator GaAs substrate. The lattice mismatch between AlSb and GaAs is about 8.5%. Therefore, the thick AlSb buffer is used as the buffer layer to prevent the dislocation propagation. Furthermore, for the integration with silicon base IC technology, the device should be realized on silicon substrate [9,10]. Therefore, the growth of GaSb(AlSb) on silicon substrate is also studied. Because of the much larger lattice mismatch and anti-phase issue, the buffer layer is much more important than that of AlSb on GaAs substrate.

Heterojunction Field Effect Transistor:

The objective of this work is to design an Sb-based heterostructure FET (HFET) with high mobility and higher breakdown voltage. In order to obtain high mobility, InAs or InSb was used as channel material. In order to further improve breakdown voltage, band gap engineering was employed to effectively enlarge the band gap of channel material. For example, by inserting a material with a larger band gap into the channel material, as shown in Fig. 2, in this schematic band diagram, we consider to insert a thin layer of GaAs into the high-mobility InAs or InSb channel to effectively enlarge the band gap of channel. The electrons' effective mass in GaAs will become smaller, because the energy level is very close to the band edge of InAs or InSb conduction band. Thus, high electron mobility can be maintained. In particular, the large valence band offset (ΔE_v) between the GaAs and InAs or InSb can be used to significantly increase the band gap of channel, which can effectively enhance the breakdown voltage. In addition, considering the requirement in lattice match, the lattice constants of InAs, InSb and GaAs are 6.06Å, 6.48Å, and 5.65Å, respectively, the very large lattice mismatch between InAs (InSb) and GaAs is at least greater than 10%, which actually will make it very difficult to grow such structure. Thus, to choose the appropriate materials with both a larger band gap and a lattice constant close to them (InAs, InSb) to enlarge the band gap of channel material is the design challenge.

From the diagram of band gap vs. lattice constant, shown in Fig. 1 [1], we can find many materials have a band gap greater than 1 eV. However, most of them have a lattice constant less than 6Å, which actually can not be used as the candidate material due to the large lattice mismatch with InAs or InSb. The materials with lattice constant ranging from 6Å to 6.5Å, including GaSb, AlSb, InAs, InSb and their alloy, are proper candidates. For InAs channel, lattice constant ranging from 6Å to 6.2 Å is the range of interest. In particular, as the lattice constant is 6.2Å, some advantages can be obtained as follows [8,11]. First, the barrier material InAlSb with Indium content (In=0.2) and the high-mobility channel material InAsSb with antimony content (Sb=0.35) are lattice-matched. Second, the barrier $\text{In}_{0.2}\text{Al}_{0.8}\text{Sb}$ and channel $\text{InAs}_{0.65}\text{Sb}_{0.35}$ formed type I heterojunction, which can avoid the problems that occurred in type II InAs/AlSb heterojunction. Besides, the strain effect plays a key role in the actual band gap as we grow material with different lattice constant. Depending on the stress type and the amount of lattice match between two different materials, the final magnitude of band gap changed significantly. Fig. 3 showed the theoretical calculation of the band gap with the quantum well lattice constant, for the case of strain quantum well on the GaSb substrate

[12]. As the lattice constant is equal to 6.2\AA , the conduction band offset (ΔE_c) and valance band offset (ΔE_v) between InAs and InAsSb are around 0.1 eV and 0.24 eV, respectively. Therefore, by inserting a thin layer of InAs layer in the middle of the InAs_{0.65}Sb_{0.35} channel, taking advantage of the large valance band offset ($\Delta E_v=0.24\text{eV}$) between InAs and the InAsSb channel, the band gap of the InAs/InAsSb composite channel can be effectively enlarged, as shown in Fig. 4.

GaSb Growth on Silicon (001) Substrate:

In this work, three samples were prepared with different buffer layer structure. After the buffer layer growth, $1\mu\text{m}$ GaSb bulk layer was grown with $1\mu\text{m/hr}$ growth rate. The V/III flux ratio was about 3 and the growth temperature was at 500°C . An 8nm In_{0.2}Ga_{0.8}Sb QW was inserted in GaSb bulk layer at 150nm below sample surface for the optical property study. The QW growth temperature was at 490°C .

The buffer layer structure in sample A, B and C is:

- A. Without any AlSb buffer layer, the GaSb was grown directly on the silicon surface.
- B. With 100nm AlSb buffer layer at 480°C , and the growth rate was $0.5\mu\text{m/hr}$.
- C. With GaSb(10nm)/AlSb(10nm) 10 periods superlattice buffer layer at 480°C , the GaSb and AlSb growth rate was $1\mu\text{m/hr}$ and $0.5\mu\text{m/hr}$.

After the growth, the sample A shows a non-mirror surface, but the sample B and C shows a better mirror surface. Therefore, the surface morphology of sample B and C is much smoother than that of sample A. Fig. 5 shows the surface AFM image of these three samples. All of the AFM image size is $10\mu\text{m}\times 10\mu\text{m}$ with 30nm scale bar. The surface roughness of sample A is the worst, and the other two samples are much similar. The surface roughness is quantified by the atomic force microscope (AFM). The root mean square surface roughness of sample B and C are 4.27nm and 3.88nm with the same scanning parameter. The sample C shows the best surface flatness quality. The flatter surface is better for the structure growth.

Fig. 6 shows the In_{0.2}Ga_{0.8}Sb/GaSb QW low temperature (20K) photoluminescence (PL) response of these three samples. The sample C shows the largest response intensity and the smallest full width at half maximum (FWHM). The FWHM of sample C is 11.2meV . The peak emission energy of the In_{0.2}Ga_{0.8}Sb QW varies from 0.71eV to 0.73eV . The peak energy variation might be due to the source beam flux variation. With simple estimation, 2% material composition difference on In_{0.2}Ga_{0.8}Sb QW results in 11meV energy level change.

Fig. 7 shows the high resolution X-ray diffraction (XRD) rocking curve from GaSb (004)

orientation of the three samples. The scatter point is the measurement data and continuous curve is the gaussian fitting curve. These three samples were measured at the same condition and the same X-ray source intensity. The sample C shows the higher intensity and smaller FWHM. The FWHM of sample C is 490 arcsec. In our study, three analysis techniques (AFM, PL and XRD) show the GaSb bulk and $\text{In}_{0.2}\text{Ga}_{0.8}\text{Sb}/\text{GaSb}$ QW quality of sample C is the best and sample A is worst. The AlSb buffer layer is necessary in the crystal growth of GaSb on Silicon substrate. Moreover, the GaSb/AlSb superlattice buffer layer is the best choice for the growth.

The lattice constant of GaSb and silicon is 6.10 Å and 5.43 Å, and the lattice mismatch is about 12%. When GaSb deposited directly on silicon substrate, it would generate many dislocations at the interface. The non-mirror surface of sample A suggests that the GaSb does not block dislocations propagation efficiently. When 100nm AlSb buffer layer was inserted at GaSb and silicon interface in sample B, the GaSb crystal shows a mirror surface. The surface AFM image of sample B is smoother than that of sample A and the PL and XRD study also shows the better result. The $\text{In}_{0.2}\text{Ga}_{0.8}\text{Sb}/\text{GaSb}$ QW PL intensity of sample B is two times larger than that of sample A. Therefore, the AlSb buffer layer plays an important role in the GaSb and silicon heterojunction growth. The lattice constant of AlSb is 6.13 Å, and the lattice mismatch to silicon is about 13%. When AlSb deposited on silicon, many dislocations generate. Observing the RHEED pattern variation during sample growth, the reconstruction pattern is spotty during the first few monolayers. The few monolayers AlSb form the QDs, which is the nucleation process, on the Silicon surface. When more AlSb deposited on the substrate, the reconstruction pattern changes from spotty to streaks. The streaky reconstruction pattern indicates that the AlSb QDs coalesce to a bulk material. This nucleation and coalescence process generates an undulation surface, which accommodates the AlSb and silicon heterointerface strain energy. These processes are the strain relief mechanism.

In sample C, the QW PL intensity shows three times larger than sample B, and the FWHM is also better than sample B. Also, the intensity and FWHM of the XRD measurement data shows the best result in the three samples. Thus, the ten periods superlattice GaSb (10nm)/AlSb (10nm) buffer layer is the best buffer layer structure to prevent the dislocation propagation in our study. The lattice constant mismatch between AlSb and GaSb is only 0.5% and thus the heterointerface is nearly strain free. The superlattice structure is able to merge dislocations and stop dislocation propagation. The first 10nm AlSb layer also plays as the nucleation and coalescence process. The 10nm AlSb layer is about 30

monolayers that are thick enough to coalesce the AlSb QDs and form the undulation surface. During the 10nm AlSb growth, the reconstruction pattern changes from spotty to streaky pattern. Fig. 8 shows the GaSb/AlSb superlattice high resolution transmission electron microscope (HR-TEM) image of sample C. In the area 1 and 2, the dislocations merge at the GaSb/AlSb interface. And, in the area 3, the dislocation stops at the interface.

Compositional Grading in GaAsSb Grown on GaAs Substrates Caused by Strain-Induced Sb Segregation:

The composition profile of GaAsSb grown on GaAs substrates by solid-source molecular beam epitaxy (MBE) has been investigated. It's found that the Sb composition fraction grades increasingly instead of keeping constant throughout the GaAsSb epitaxial layer. This is attributed to the strain-induced Sb segregation during the growth of GaAsSb on the GaAs substrate.

Epitaxial growth of GaAsSb/GaAs heterostructures for the applications of long-wavelength light-emitting devices is a critical issue because of the significant lattice mismatch between GaAsSb and GaAs. In this work, the samples were grown by MBE on GaAs (100) substrates. A GaAsSb layer, which has different thicknesses (10, 20, 30, 40, 60, 120, and 200 nm) for different samples, was grown at 505 °C on top of a 200-nm GaAs buffer.

X-ray reciprocal space mapping (RSM) around the GaAs (224) reflection was performed to estimate the degree of lattice relaxation and the peak Sb composition of the GaAsSb layer, as shown in Fig. 9. The 10-nm GaAsSb layer is found fully strained and has the in-plane lattice constant the same as that of the GaAs substrate. With the thickness more than 10 nm, the GaAsSb layer becomes partially relaxed and the in-plane lattice constant increases with the layer thickness. Mathematical analysis of the RSM pattern gives the amount of relaxation and the peak Sb composition, as shown in Fig. 10 and 11, respectively. Also shown in Fig. 11 is the peak Sb composition determined from Rutherford backscattering spectrometry (RBS) measurements, which in this work use a 4-MeV C^{2+} beam instead of He^+ to achieve a better resolution. RSM and RBS both show that the peak Sb composition of the GaAsSb layer increases with increasing the layer thickness. The depth profile of the Sb composition shown in Fig. 12 is extracted by numerically fitting the experimental RBS data. The Sb composition, instead of staying constant, is found to grade increasingly toward the surface. Strain-induced Sb segregation in the GaAsSb layer grown on the GaAs substrate is considered to account for

the observed result. During the growth of GaAsSb on GaAs, the compressive strain imposed on the GaAsSb layer tends to propel the Sb atoms to segregate upward. In this way, the strain-associated energy in GaAsSb is lowered.

We have also used the ion channeling technique to investigate the vertical distribution of strain inside the GaAsSb layer. For the ion channeling curve of the 30-nm sample (Fig. 13(a)), the Sb signal and the GaAs signal nearly overlap, indicating that the GaAsSb layer is fully strained. For the 90-nm sample (Fig. 13(b)), the Sb signal of the GaAsSb layer at the surface shows a noticeably narrower full width at half maximum (FWHM) than that near the GaAsSb/GaAs interface. This is an indication that the strain is larger in the GaAsSb layer near the surface.

Reference:

- [1] B. R. Bennett, R. Magno, J. B. Boos, W. Kruppa and M/ G. Ancona, Solid-State Electron **49**, 1875 (2005)
- [2] B. Brar and H. kroemer, IEEE Electron Device Lett. **16**, 548 (1995)
- [3] C. R. Bolognesi, M. W. Dvorak, and D. H. Chow, IEEE Trans. Electron. Device **46**, 826 (1999)
- [4] C. R. Bolognesi, and D. H. Chow, IEEE Electron. Device Lett. **17**, 534 (1996)
- [5] J. B. Boos, M. J. Yang, B. R. Bennett, D. Partk, W. Kruppa, C. H. Yang and R. Bass, Electron. Lett. **34**, 1525 (1998)
- [6] H.-K. Lin, C. Kadow, M. Dahlström, J. -U. Bae, M. J. W. Rodwell, A. C. Gossard, B. Brar, G. Sullivan, G. Nagy, and J. Bergman, Appl. Phys. Lett. **84**, 437 (2004)
- [7] H.-K. Lin, C. Kadow, J. -U. Bae, M. J. W. Rodwell, A. C. Gossard, B. Brar, G. Sullivan, G. Nagy, and J. Bergman, J. Appl. Phys. **97**, 024505 (2004)
- [8] J. B. Boos, M. J. Yang, B. R. Bennett, D. Partk, W. Kruppa and R. Bass, Electron. Lett. **35**, 847 (1999)
- [9] K. Akahane, N. Yamamoto, S. Gozu, and N Ohtani, J. Crystal Growth **264**, 21 (2004)
- [10] G. Balakrishnan. S. Huand, L. R. Dawson, Y. C. Xin, P. Conlin, and D. L. Huffaker, Appl. Phys. Lett. **86**, 034105 (2005)
- [11] M. J. Yang, B. R. Bennett, M. Fatemi, P. J. Lin-Chung, W. J. Moore and C. Y. Yang, J. Appl. Phys. **87**, 8192 (2000)
- [12] C. E. Pryor and M. E. Pistol, Phys. Rev. B **72**, 205311 (2005)

Figure caption:

1. The diagram of energy gap and lattice constant, with lattice constant ranging from 5.4Å to 6.5Å.
2. The schematic band diagram of the ideal channel structure. The channel consisted of the high mobility channel layer InAs or InSb and a large band gap layer, for example, GaAs.
3. Band edge diagram of alloyed strained wells on GaSb (ref. 4).
4. The schematic band diagram of the designed channel structure. The composite channel consisted of the high-mobility InAs and InAsSb channel layer, where the middle InAs layer was used to enlarge the band gap of the channel.
5. The surface AFM image of these three samples. The image size is 10µm×10µm with the 30nm scale bar.
6. The 20K PL response from the 8nm In_{0.2}Ga_{0.8}Sb/GaSb QW. The FWHM of sample C is 11.2meV.
7. High resolution XRD (004) rocking curve of GaSb on Silicon. The FWHM of the sample C is 490 arcsec.
8. Cross-section HR-TEM image of the GaSb/AlSb superlattice on silicon substrate in sample C. In area 1, 2 and 3 the dislocations merge or stop at the superlattice interface.
9. RSM measurements taken at the GaAs (224) reflection for the samples with the GaAsSb buffer layer of (a) 10 nm, (b) 30 nm, (c) 60 nm, (d) 200 nm
10. Amount of relaxation of the GaAsSb layer in the samples with various GaAsSb thicknesses.
11. The peak Sb content of the GaAsSb layer in the samples with various GaAsSb thicknesses.
12. The grading profile of the Sb content in the GaAsSb layer.
13. Ion channeling results show that the elements located at different vertical positions in the GaAsSb layer are subject to different stresses.

Figure 1

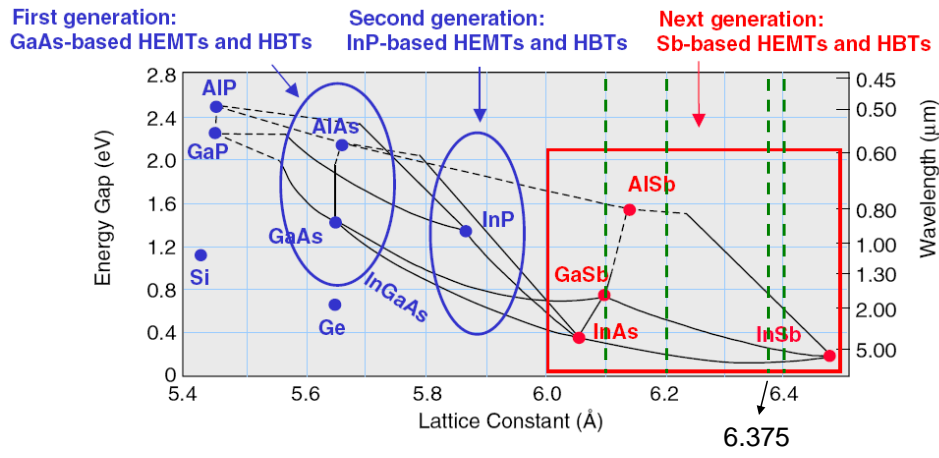


Figure 2

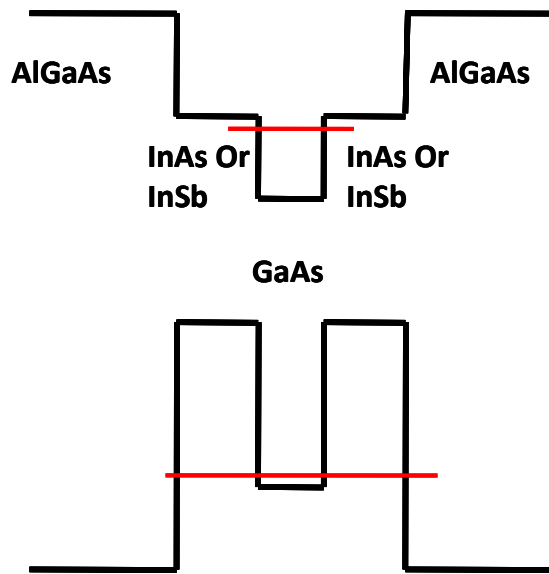


Figure 3

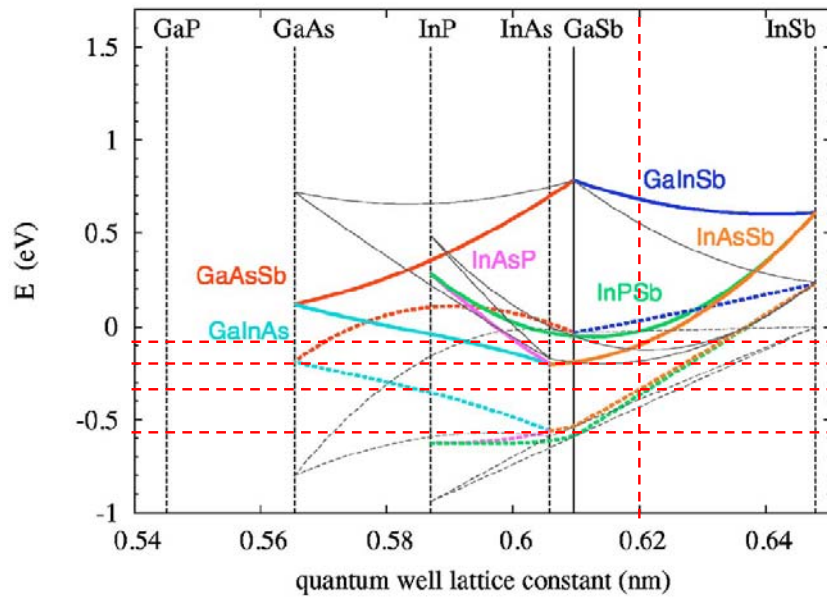


Figure 4

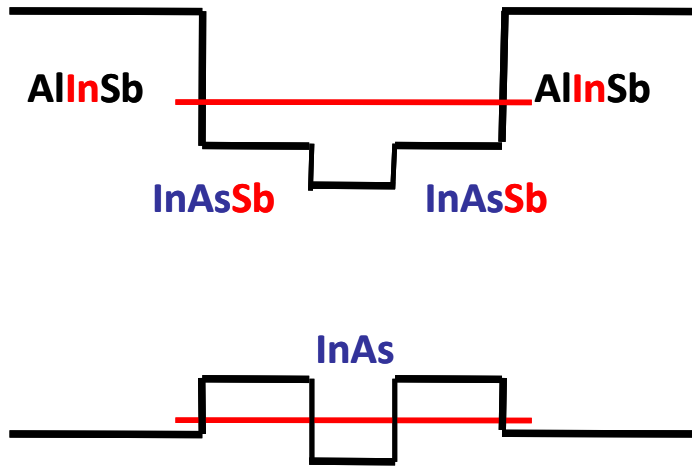


Figure 5

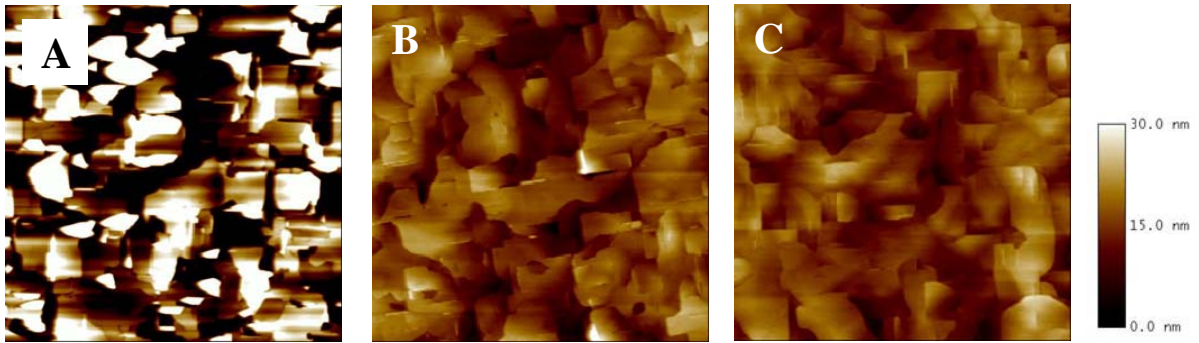


Figure 6

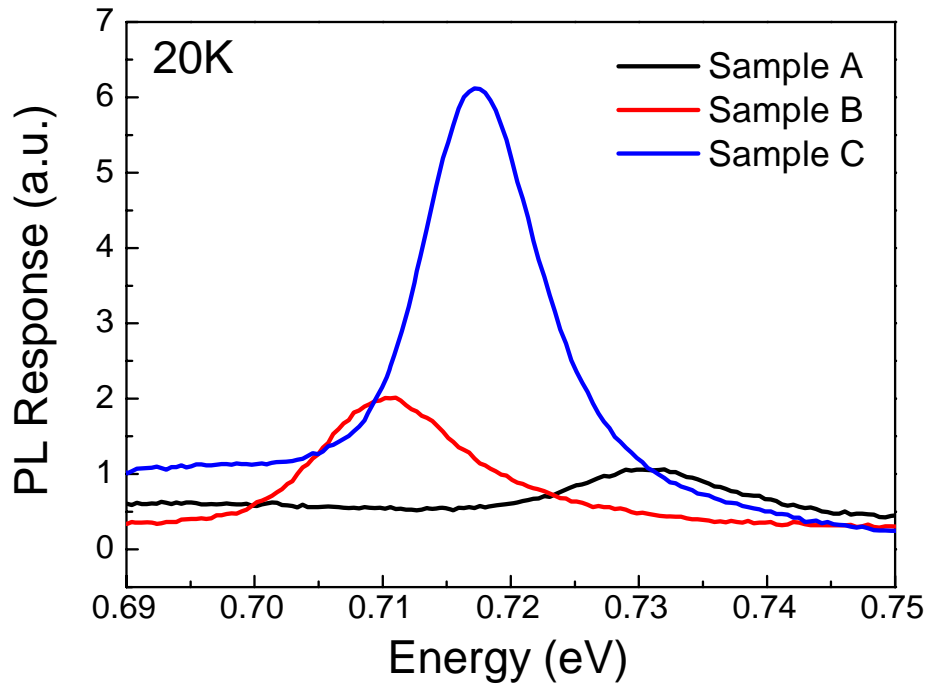


Figure 7

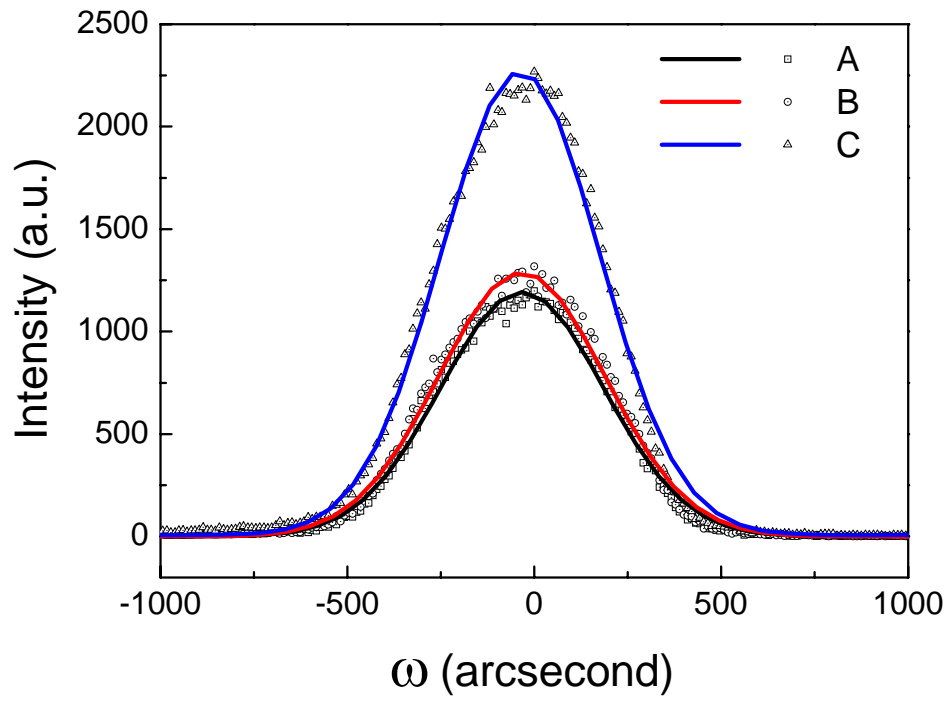


Figure 8

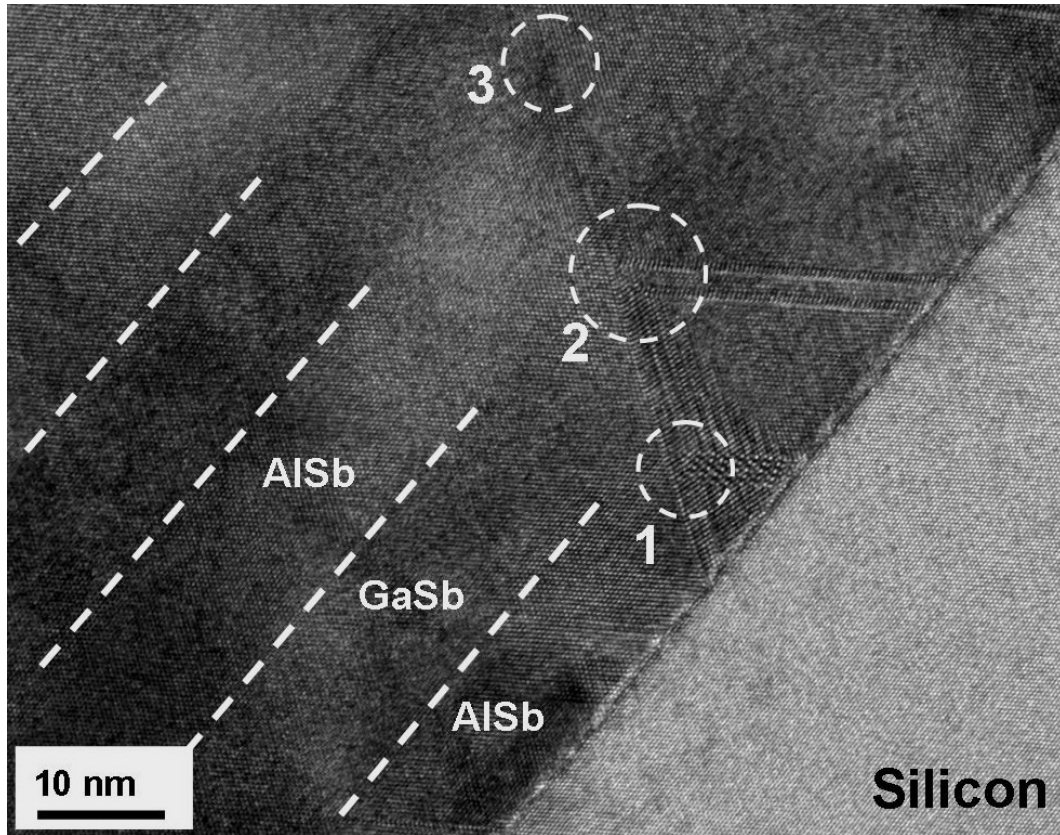


Figure 9

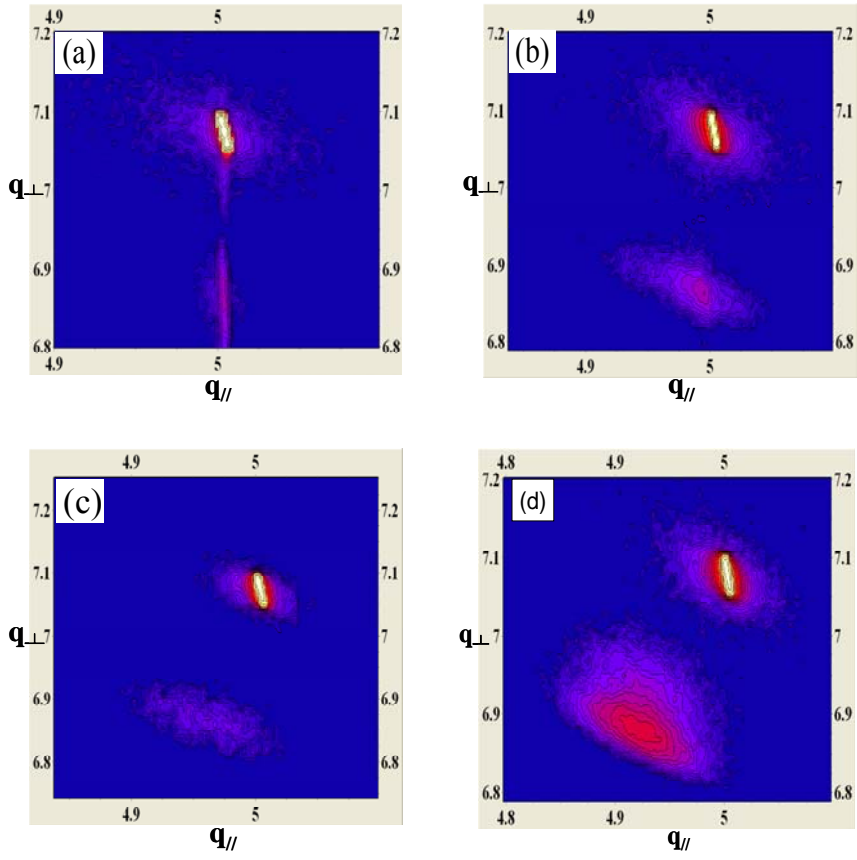


Figure 10

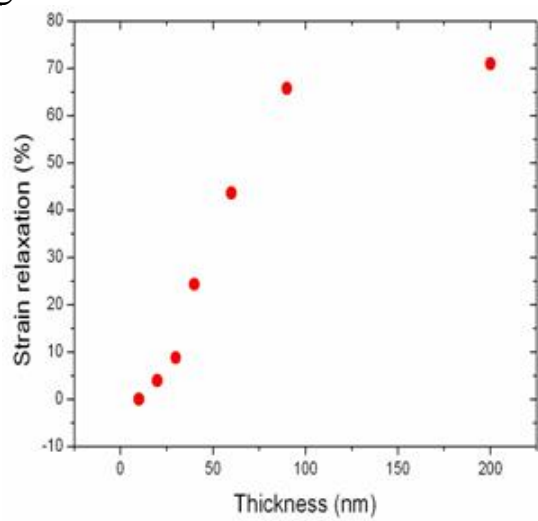


Figure 11

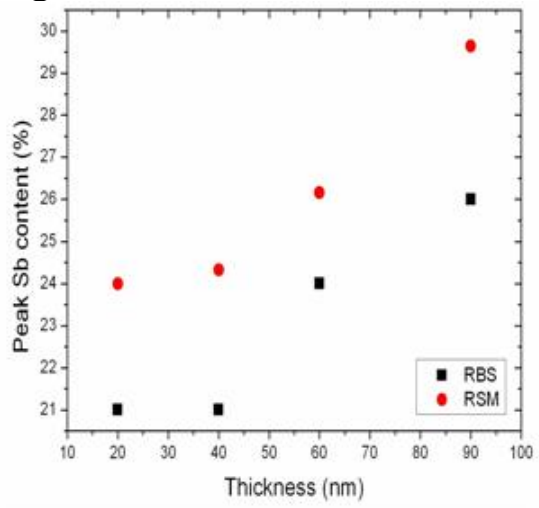


Figure 12

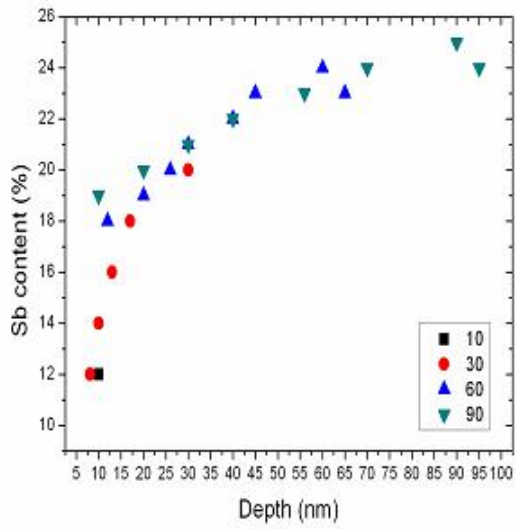


Figure 13

